Characterization and Modeling of the Deformation and Failure Behavior of Neat Thermoplastic Homopolymers under Impact Loading Conditions

P. S. Stelzer[1], Z. Major[1]

[1]Institute of Polymer Product Engineering, Johannes Kepler University Linz, Austria

Summary

The increasing use of thermoplastic polymers in structural applications exposed to impact loading conditions drives the need of accurate and reliable FEM simulations. Classical elasto-plastic formulations are based on the von Mises yield criterion and only of limited suitability for modeling polymers. Advanced material models become necessary to capture the complex mechanical deformation and damage behavior. However, the experimental effort is significantly higher to provide material input data. The objective of this study was the modeling of the deformation and damage behavior of thermoplastic homopolymers under monotonic and impact loading conditions with the commercial FEM code LS-Dyna. For this purpose, the use of the material model SAMP-1 and the damage model GISSMO for a Polypropylene and a Polycarbonate grade was investigated.

A comprehensive experimental characterization, applying full-field strain analysis using a digital image correlation technique and a high speed camera, was performed for the calibration of the models. To derive the input parameters for SAMP-1, uniaxial tensile and simple shear tests were carried out. Experimental compression data was taken from previous studies. Coupon tests were conducted to assess the stress triaxiality dependent damage and failure behavior. To describe the actual local deformation behavior and to provide a straight-forward methodology, a direct experimental approach was favored to derive the material model input data. Validation was performed on the tensile tests by comparing the numerical and experimental results of the global force-displacement curves and of the local deformations.

The elasto-viscoplastic constitutive model SAMP-1 was calibrated for ambient temperature (23 ± 1 °C) and different strain rates (0.0002, 0.1, 1, 10 and 100 s^{-1}). Until the yield point is reached, the mechanical response is linear elastic. The characteristic pressure dependent quadratic yield surface of SAMP-1 was fitted by the input of tensile, compression and shear data. Moreover, the model incorporates multiaxial hardening behavior. The non-isochoric plastic deformation could be captured by the experimentally determined apparent Poisson's ratio.

The determination of the failure curve, in terms of failure strains as a function of the stress triaxiality factor, is essential for the calibration of ductile damage models like the formulation implemented in SAMP-1 or GISSMO. A combined experimental-numerical approach was used to identify equivalent plastic strain values and corresponding stress triaxiality factors at fracture initiation. The method of an average triaxiality factor was selected as a rather direct way to extract the failure strains from the experimental tests.

Keywords

Polymers, DIC, Impact, SAMP-1, GISSMO

1 Introduction

In this study, the deformation and failure behavior of thermoplastic homopolymers under monotonic and impact loading conditions was modelled using LS-Dyna. The LS-Dyna version R8.1.0 was used to carry out the FEM simulations. SAMP-1 (Semi-Analytical Model for Polymers) was selected to capture the complex multiaxial deformation behavior. It is one of the currently most advanced material models implemented in commercial FE codes.

Optical strain measurement techniques for the successful calibration of SAMP-1 material cards were used successfully in recent works. Lin et al. [1] used the measured multiaxial true stress curves of a talc-filled PP directly as input for the material card. Engineering stress-strain data were used to compute the true stress-true strain input curves by Lobo et al. [2]. Nutini et al. [3] followed the effective stress notion and used constant volume stress values in conjunction with a damage parameter calculated by means of the volumetric strain. Also Dayan et al. [4] used effective stress values and a damage parameter measured by uniaxial tensile loading-unloading tests.

A comprehensive experimental characterization is necessary to obtain a reliable and accurate input data set for the calibration of the material and damage models. Apart from the usually adopted uniaxial tensile test data, additional experiments are required to calibrate the complex material cards. To describe the actual local deformation behavior and to provide a straight-forward methodology, a full-field strain analysis by using a digital image correlation (DIC) technique was applied to derive the material parameters directly from the experimental results.

The stress triaxiality dependent failure was investigated by determining the failure locus in terms of equivalent plastic strain at failure vs. stress triaxiality factor (here also refered to as failure curve). The failure curve is essential for the calibration of ductile damage models like the formulation implemented in SAMP-1 or GISSMO (General Incremental Stress State Dependent Damage Model). Many authors followed an inverse engineering methodology for the generation of the failure curve for metals [5, 6] and polymers [1, 7]. A combined experimental-numerical approach was used to identify equivalent strain values and corresponding stress triaxiality factors at fracture initiation, respectively.

2 Experimental Characterization

To provide the input parameters for the material model SAMP-1, uniaxial tensile tests and shear tensile tests were carried out. Compression test data was taken from previous studies [8]. For the determination of the failure curve so called coupon tests were conducted to assess the stress state dependent failure behavior. The temperature dependency was not investigated, all tests were conducted at room temperature (23 ± 1 °C).

The mechanical tests were carried out on a servo-hydraulic testing machine of MTS Systems Corporation (Eden Prairie, MN, USA). For the low rate test setup the Aramis 4M Camera System of GOM GmbH (Braunschweig, Germany) was utilized to record the test images. The high speed camera Phantom v711 of Vision Research Inc. (Wayne, NJ, USA) was used for the impact tests. Out of experience a frame rate of maximum 100,000 Hz with accurate and reliable results can be reached in the case of the uniaxial tensile test.

2.1 Materials and Specimens

Two different commercial materials, the semi-crystalline Polypropylene (PP) and the amorphous Polycarbonate (PC), were examined in this work. The PP grade from the company Borealis AG (Linz, Austria) was manufactured and delivered in form of injection molded plates (205 x 145 x 4 mm). The PC grade of Covestro AG (Leverkusen, Germany) was provided in form of injection molded multipurpose specimens of Type 1A according to ISO 527/2012 and injection molded plates (400 x 300 x 4.5 mm).

Four different specimen geometries were adopted in this investigation. The standard multipurpose specimen according to ISO 527-2 was used to derive the uniaxial tensile properties. The coupon test specimens, to cover a wide range of positive stress triaxiality factors, include miniflat, notched and shear tensile specimens. To account for the strong rate dependency, a method of different test velocities was chosen to compare the various sample geometries. Regarding a characteristic

deformation length of the tensile bars (see Figure 1), a series of constant cross head speeds was selected to ensure equal nominal strain rates.
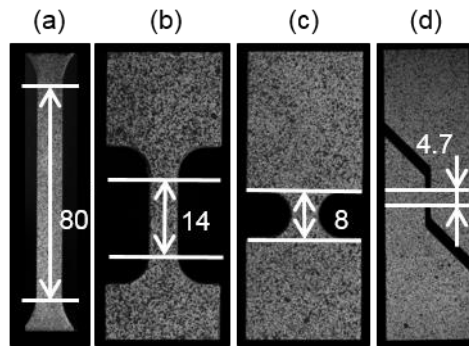
Fig.1: Investigated tensile test specimens with characteristic deformation lengths (in mm): (a) multipurpose, (b) miniflat, (c) notched, (d) shear.

All sample geometries were milled out of the provided injection molded plates in direction to the melt flow. The injection molded multipurpose specimens were used for the uniaxial tensile testing of the PC. Anisotropic effects of the mechanical behavior caused by the semi-crystalline morphological structure of PP were not part of this study. No anisotropic effects were expected for PC due to its amorphous structure.

2.2 Local Full-field Strain Measurements

Not only the longitudinal but the full 2D multiaxial strain fields were measured on the surface of the samples with the DIC system. Data reduction techniques were then applied to obtain the true stress-true strain relations for tensile and shear. The true strain values at each time stage were calculated with the DIC software Aramis by the mean average value over a defined measuring area. For a uniaxial tensile test the strain analysis can be applied on a global and a local scale, depending on the choice of the measuring area, as depicted in Figure 2 (left). However, due to the inhomogeneous deformation behavior of polymers associated with strain concentration and neck propagation along the sample length, the global strain determination is not suitable. For an accurate description of the true deformation behavior and to capture the strain localization effects, the strains need to be assessed locally in the necking zone [9].

The influence of different gauge lengths of the measuring area over the width of the multipurpose specimen was studied on the PC grade. This sensitivity study is shown on the uniaxial tensile test with a testing speed of 1 mm/min. For the local measurement in the necking zone a gauge length of 1, 4 and 8 mm was chosen. The strains were also calculated on a global scale with a gauge length of 80 mm. The resulting true stress-true strain curves are depicted in Figure 2 (right). For the global strain measurement a strong strain softening effect with a sudden load drop could be observed. Since the strain localization was not captured, the strain values are significantly lower than for the local evaluations. With decreasing gauge length a smoother transition between strain softening and cold drawing phase can be seen. This example shows the signifance of capturing the true, local deformation behavior of polymers by adequate testing methods.
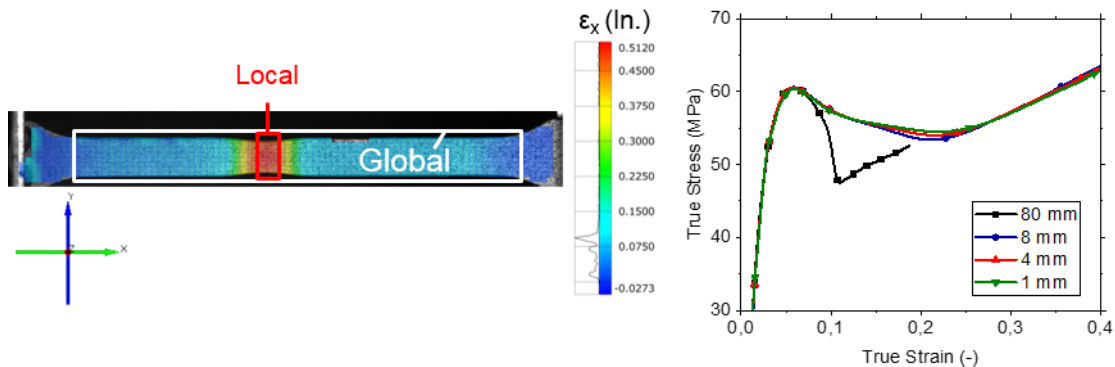
Fig.2: Sensitivity study on the size of the measuring area with different gauge lenghts.

2.3   Tensile Tests

To evaluate the true stress–true strain relations of the tensile test data the actual cross section during deformation has to be considered. The reduction of the cross section can be assessed with the transverse strain ε_t. The transverse strains in width and thickness directions were assumed to be equal [10]. The corresponding true stress values σ were then calculated at each strain stage:

$$\sigma = \frac{F}{A} = \frac{F}{A_0 (1 + \varepsilon_t)^2} \tag{1}$$

where F is the measured force. A and A_0 denote the actual and initial cross section. To account for the strong rate dependency tensile tests were conducted at a quasi-static test velocity of 1 mm/min and at elevated test speeds of 8, 80 and 800 mm/s. Additional measurements at 8 m/s for PP and at 50 mm/min for PC were examined. These test velocities correspond to nominal strain rates ranging from 0,0002 to 100 s^{-1}. The local true stress - true strain curves are shown in Figure 3. For PC no accurate results could be obtained at 800 mm/s.
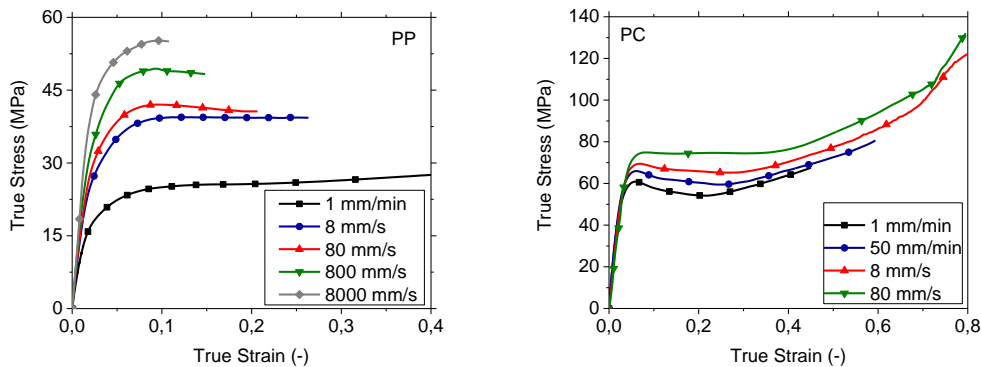
Fig.3:   *Local true stress-true strain curves for the PP (left) and PC (right) at different testing speeds. Last point marks the failure point at elevated test speeds > 50 mm/min.*

The yield stress values were determined from the averaged stress curves. Various methods exist to define the yield point for materials, like offset methods or using the first peak value in the stress-strain relation [11]. The Considère's Construction [12] was believed to be the most suitable approach to define the yield point for polymers in this study. The yield stress σ_y was determined by the following criterion:

$$\sigma = \frac{d\sigma}{d\varepsilon} \tag{2}$$

Quinson et al. conducted uniaxial tensile tests of PC and determined the exact yield point via residual strain measurements after unloading [13]. Considering this study, it was found that the instability criterion after Considère given by equation (2) was accurate to evaluate the real yield point.

2.4   Shear Tensile Testing

To describe the shear deformation behavior a geometry of a shear tensile test specimen was employed according to [14]. It is a modified shear specimen geometry based on the standard ASTM B831 to realize a planar simple shear test condition. To obtain the shear stress - strain curve the local shear strain values ε_{xy} were measured by DIC. In Figure 4 the local measuring area over the shear deformation zone (marked by the black rectangle) is displayed. On the tips of the shear zone relatively high normal strains were observed. Therefore, they were not included in the measuring area.

The shear yield point was determined after Considère with equation (2), respectively to the uniaxial standard tensile test. It could be confirmed by DIC measurement, that a simple shear condition was ensured to a high degree (see Figure 5). The vertical black line marks the shear yield point after Considère. Until reaching instability a high degree of the simple shear condition was ensured. That means the employed tensile shear tests were accurate to determine the shear input data. The yield

point is followed by strain localization and plastic flow. This is usually associated with a complex stress state.
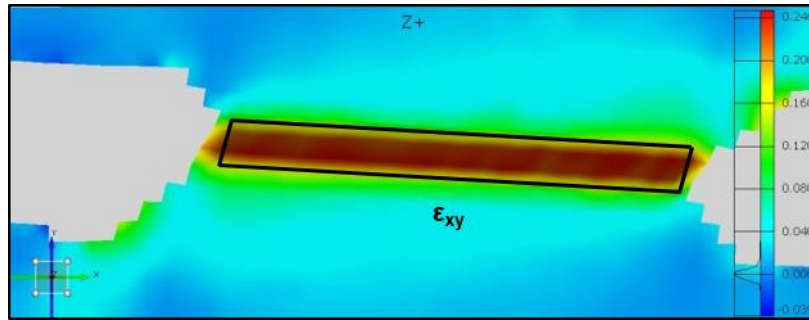
Fig.4:   Local measurement of the shear strain ε_{xy} by DIC.
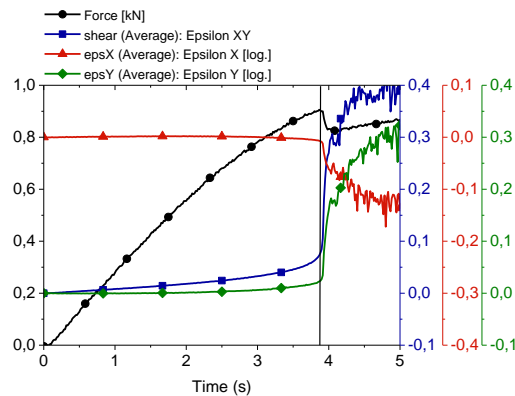
Fig.5:   DIC strain analysis of the shear tensile test on the example of PC.

3   Calibration of the Material Model SAMP-1

SAMP-1 uses the tabulated load curves exactly, with the advantage that the test results are directly reflected [15]. But on the other hand this leads to the need of an accurate and reliable experimental characterization.

3.1   Multiaxial, Non-isochoric Deformation Behavior

Regarding the choice of the elastic modulus and hence the definition of the virtual yield point two approaches are followed to model the onset of plastic deformation. Often a virtual yield point is defined to capture the onset of non-linear elastic behavior in numerical simulations. This virtual yield point has a much lower stress value than the physical one. This is especially important to model the impact energy absorption behavior if the elastic part is big compared to the total deformation. This approach was employed for the examined PP grade, since we observed a strong non-linear viscoelastic deformation behavior. Accordingly, the tensile modulus is defined by 90% of the mean average value of the measured Young's moduli at the different testing rates.

On the other hand, the tensile modulus in SAMP-1 could be defined as a secant modulus until the yield point after Considère´ to reflect the plastic strain as realistic as possible. This second approach was used for PC. This modeling technique is reasonable, if the elastic part is small compared to the total deformation and if the constitutive model represents the actual material behavior. A similar modeling approach can be found in [16].

The pressure dependent quadratic yield surface of SAMP-1 and the anisotropic hardening was modeled by the input of a tensile, compression and shear yield curve. The multiaxial yield curves were generated from the quasi-static data set at the nominal strain rate of 0.0002 s^{-1}. The difference of the choice of the elastic modulus for both materials can be seen clearly in Figure 6. Strain rate dependency was included by input of multiple tensile yield curves at various test velocities (Figure 3).

A constant strain rate during tensile deformation according to nominal values was assumed. The effect of temperature on the constitutive relation is not considered by SAMP-1.
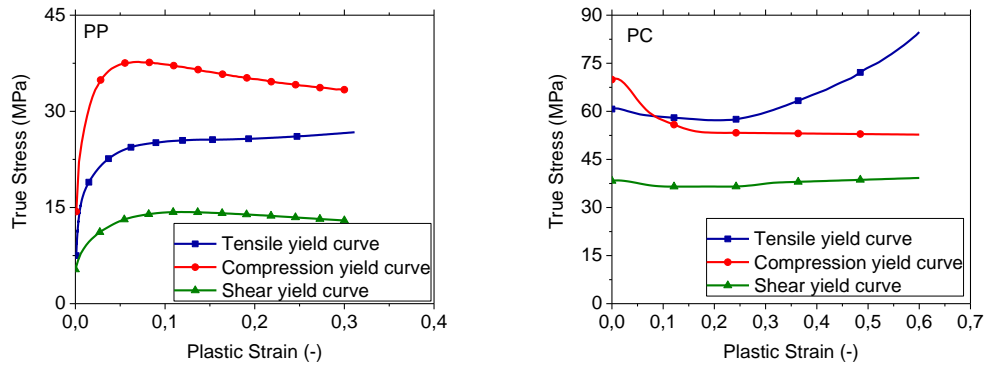
Fig.6:   Quasi-static input set of multiaxial yield curves of PP (left) and PC (right).

With the definition of the plastic Poisson's ratio v_p the non-isochoric plastic deformation can be described in the model. The plastic Poisson's ratio was evaluated by data reduction of the experimental DIC data from the uniaxial tensile test at quasi-static test velocity. The longitudinal and transverse strains respective to their time dependency were regarded. The plastic Poisson's ratio and the corresponding tensile yield curve are displayed in Figure 7.
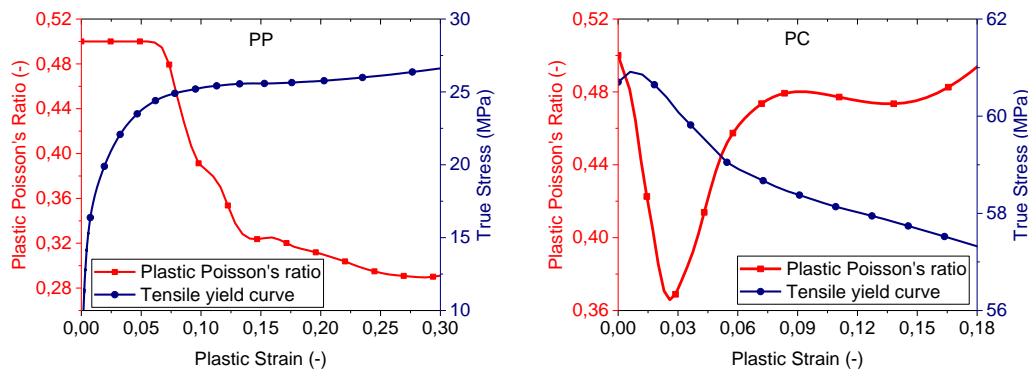
Fig.7:   Plastic Poisson's ratio and true stress vs. plastic strain of PP (left) and PC (right).

For both materials a constant plastic Poisson's ratio of 0.5 was assumed for the plastic strains in compression. As theoretically postulated a value of 0.5 is observed at the tensile yield point [2]. Since the virtual yield of PP was set to a lower stress value, v_p was kept constant with a value of 0.5 until the physical yield point. After that point a sudden drop was determined reaching an asymptotic value of 0.29. For PC a sudden drop of the plastic Poisson's ratio from a value of 0.5 to its elastic value of 0.37, coinciding with the strain softening effect and necking, was measured. With the propagation of flow localization along the specimen axis v_p increases again, until a constant value of 0.5 in the cold drawing phase. A similar shaped curve of v_p for PC was found in [17], by a stage-wise optimization method of the uniaxial yield curve and the plastic Poisson Ratio. This fact encourages the direct determination of the plastic Poisson's ratio by DIC as followed in this work. On the basis of these measurements the assumption of a constant plastic Poisson's ratio would be too simplistic.

3.2   Effective Stress Concept and Damage Modeling

An isotropic, scalar ductile damage model based on the phenomenological concept of effective stress proposed by Lemaitre [18] is implemented in SAMP-1. A tabulated load curve of the damage parameter d as a function of the plastic strain ε_p under quasi-static uniaxial tension has to be provided. The yield stress and elastic modulus is affected by d [15]. The effective stress σ_{eff} is defined as the force F divided by the effective cross section A_{eff}:

$$\sigma_{eff} = \frac{F}{A_{eff}} = \frac{F}{A(1-d)} = \frac{\sigma}{1-d} \tag{4}$$

with σ as the true stress and A the actual cross section of the material. The effective cross section equals the true (total) cross section minus the area of intersecting voids and cracks in the damaged state. The constant volume approximation to derive the stress values, as used for metals is in general not a suitable conversion method for polymers. Therefore, the true stresses σ were generated using equation (1) to account for the non-isochoric deformation behavior. However, with the definition of the effective stress concept, it can be assumed that the volume of the undamaged material remains constant during deformation. The effective stress σ_{eff} can then be identified with the constant volume stress σ_{cv} according to Nutini et al. [3]. The constant volume stress (CV stress) can be calculated at each strain stage with:

$$\sigma_{cv} = \sigma_N (1 + \varepsilon_N) \tag{5}$$

where σ_N and ε_N are the nominal stress and nominal strain. With this concept of effective stress and equation (4) the measured true stress values σ and the effective stress values σ_{cv} can be used to calculate a damage load curve $d(\varepsilon_p)$. This simple derivation of the damage parameter yields similar values like the calibration method of the damage parameter on the volumetric strain in [3].

4 Validation of SAMP-1

Validation was performed on the experimental results of the tensile tests. Globally, the FE results were compared to the experimental force-displacement curves. On a local scale, the strain values and deformation patterns were compared. A validated material card is essential for the subsequent determination of the ductile failure locus.

Due to the planar geometry, the tensile specimens can be idealized as 2D models using symmetry conditions and quadrilateral shell elements for the meshing. With respect to damage and failure modeling, the shell approach is useful to remove the lode angle parameter from consideration in the simulations. Fully integrated, linear shell elements of type 16 were used. An element size of 1 mm was chosen as a compromise between the computational costs and the accuracy of the results.

4.1 Validation Results for PP

On the basis of the preceding procedure a suitable calibration method of SAMP-1 for PP was found. The CV stress can be used as effective stress values in conjunction with a damage parameter assessed on the relation between effective and true stress values. The CV stress values defining the tensile yield curves were generated at each testing rate. A simple scaling of the quasi-static curve was not adequate to describe the strong rate dependency of PP. However, the multiaxial hardening curves were scaled on the quasi-static tensile yield curve. The solutions were not stable for the experimentally determined compression and shear data. For compression a scaling factor of 1.5 and for shear a factor of 0.63 were applied, according to the measured yield stresses.

In Figure 8 the force-displacement curves of the tensile testing of the miniflat and notched specimens at different nominal strain rates according to the characteristic deformation lengths are shown. The experimental results are given for validation.
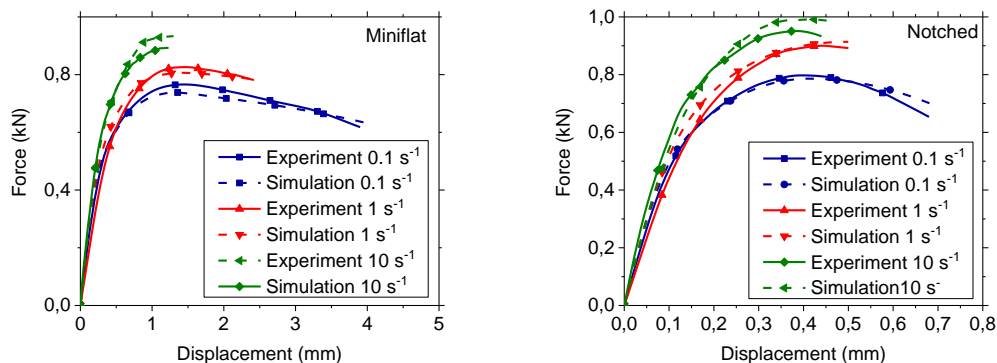
Fig.8: Validation of the miniflat (left) and notched (right) tensile tests at various nominal test rates.

The local strains of the calibration independent coupon tests (miniflat and notched) were investigated at a nominal testing rate of 10 s^{-1}. The full-field strain measurements by DIC on the surface of the specimens were used for the qualitative validation of the FEM models. As quantitative criterion the maximum strain value of the simulation was compared to the experiment. The results are shown at the displacements at failure in Figure 9.
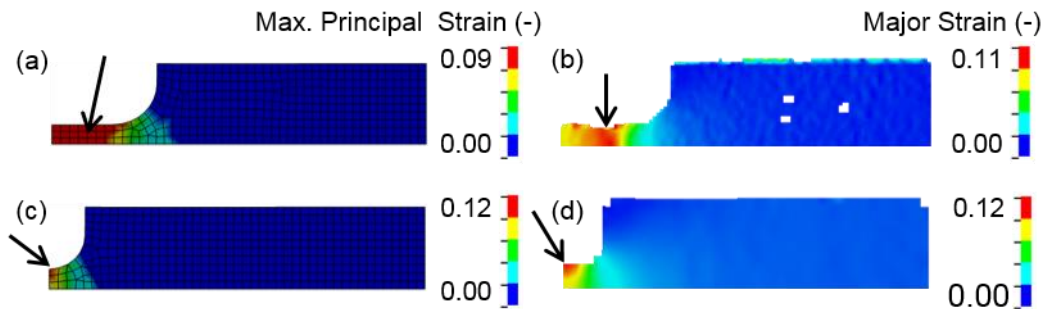
Fig.9: *Total strain of the coupon tests at a nominal strain rate of 10 s^{-1}. Arrows mark the locations of maximum values. (a) FEM miniflat, (b) DIC miniflat, (c) FEM notched, (d) DIC notched.*

The locations of the simulated maximum strain values and the strain distribution pattern coincide with the measured ones. But the experimental strains with a maximum averaged value of 11 % in the miniflat tensile test are more localized as against to the FEM model. Since the anisotropy due to crystalline domains in PP was not taken into account, the simulated strains were nearly equal across the ligament area.

4.2 Validation Results for PC

The CV stress values differ only slightly from the measured true stress values, resulting in a minor difference of the global force-displacement responses (Figure 10, left). Since the principal microscopic deformation mechanism of PC (without crack-like defects) is shear yielding, a nearly isochoric deformation behavior is reasonable. Thus, the true stress values are preferred since the transverse strain are included representing the real local deformation behavior (Figure 10, right).
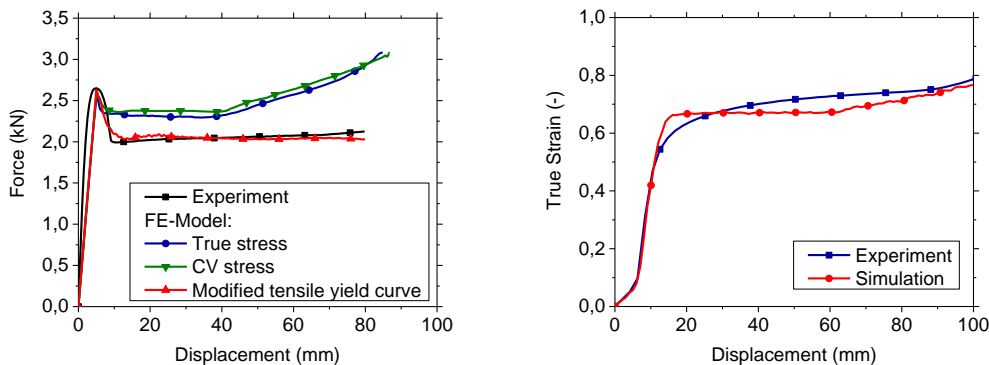
Fig.10: *Uniaxial tensile test results at 8 mm/s: Force vs. displacement (left) and local true strain vs. displacement (right).*

However, the load drop at necking was not captured satisfactorily for the uniaxial tensile test. No damage parameter was defined. The reason therefore is, that by using a damage parameter the local deformation behavior was not matched accurately. The same was true for a modified tensile yield curve to predict the load drop in the uniaxial tensile test (see Figure 10). Apart from that, a damage parameter fitted on the uniaxial tensile test would also not predict sufficiently the load drop in the coupon tests due to the stress state dependent failure behavior. The failure curve is then calibrated on the "undamaged" material model and the obtained values of plastic failure strains and stress triaxiality factors are considered representable of the actual behavior. A non-linear, stress triaxiality dependent damage evolution law by GISSMO is proposed to model the stress state dependent load drop in the coupon tests.

Contrary to the calibration of PP, the compression and shear yield curves were not scaled on the tensile curve. A parameter study showed that the best results were obtained by using the experimentally measured multiaxial hardening curves. The rate dependent tensile yield curves could be easily scaled according to Figure 3 for PC.

5 Determination of the Failure Curve

To obtain the limiting fracture curve in the equivalent plastic strain and stress triaxiality space a series of material tests with different geometries need to be performed. In this work 3 coupon tests with a selected range of stress triaxiality factors from 0 (pure shear) until 0.4 (notched tensile specimens) were investigated. A miniflat, notched and shear tensile specimen geometry were selected accordingly to [6]. Exemplary failure curves at a nominal strain rate of 10 s^{-1} were generated for PP and PC.

The introduction of an averaged triaxiality factor makes the determination of the failure curve a straight-forward process. The location of ductile fracture initiation and the displacement to fracture were identified from experimental observations and simulations. Then, from each coupon test a single value of equivalent plastic strain at failure $\varepsilon_{p,f}$ and its corresponding average stress triaxiality factor η_{av} were identified. This method can be found in [5]. The average stress triaxiality factor η_{av} is defined by:

$$\eta_{av} = \frac{1}{\varepsilon_{p,f}} \int_{0}^{\varepsilon_{p,f}} \eta(\varepsilon_p) d\varepsilon_p \tag{6}$$

The evolution of the stress triaxiality factor η as a function of the equivalent plastic strain ε_p in the critical elements is shown at the nominal strain rate of 10 s^{-1} in Figure 11.
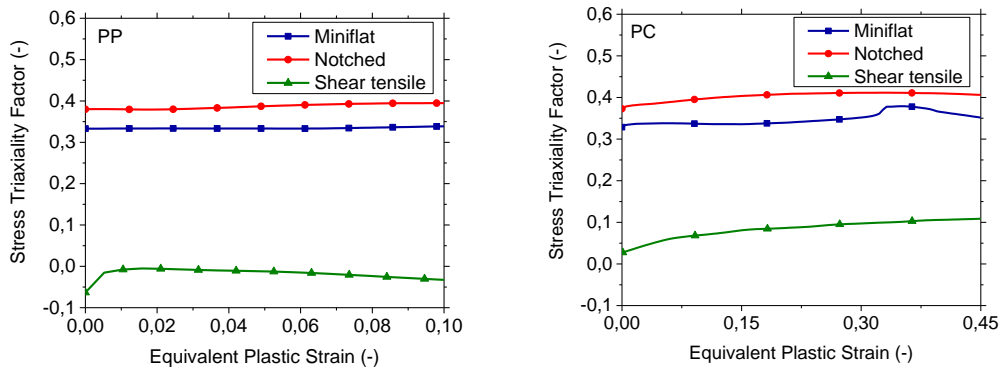
Fig.11: Evolution of the stress triaxiality factor η as function of the equivalent plastic strain at a nominal strain rate of 10 s^{-1} for PP (left) and PC (right).

For the miniflat and notched tensile test the triaxiality factor did only vary little until ductile failure initiation, which justifies the method of the average stress triaxiality factor. For the shear tensile test no state of pure shear was reached in the simulation contrary to the experimental measurements. The FEM model was not able to predict the strong ductile deformation in that case. This caused numerically element deletion prior to reaching the experimental failure displacement. The predicted plastic strains in the critical elements reached values of over 150 % before their deletion. The examined PP and PC grades are thus not likely to fail in shear mode at the considered test rate. This was confirmed by experimental observation. An arbitrary chosen high value of $\varepsilon_{p,f}$ for a triaxiality factor of 0 (pure shear) is therefore proposed.

In [1] a numerical optimization procedure was employed to identify a failure curve for a PP grade with a quadratic fit. A quadratic polynomial function was also used here to fit the directly evaluated failure points and to provide an exemplary limiting fracture curve for the examined materials at 10 s^{-1} (Figure 12).

For a biaxial tension stress state (η = 2/3) a value of 3.2 was proposed for the equivalent plastic failure strain in a study about failure behavior of a PP employing puncture tests [19]. Out of experience, a high value could be also chosen for compression (η < 0) to not reach failure in that stress state. This

information together with the determined failure points make the use of a quadratic fit reasonable to model the stress state dependent failure in the examined range of stress triaxiality factors.
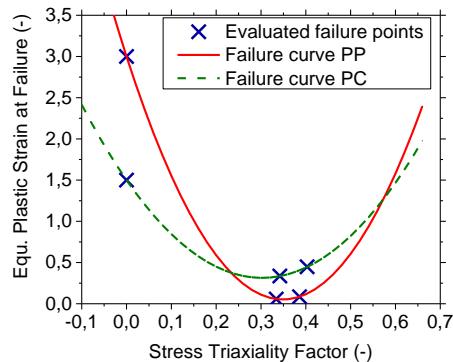
Fig.12: Exemplary failure curve at a strain rate of 10 s⁻¹. Quadratic polynomial fits and single failure points by average triaxiality for PP and PC.

6 Conclusions

The direct experimental determination of the input data set by means of DIC was effective and straightforward for the calibration of SAMP-1 for PP and PC. The actual, local deformation behavior and true stress – true strain relations could be captured accurately by the simulation models. SAMP-1 was found to be a suitable material model for thermoplastic homopolymers. Our models incorporate viscoplastic and multiaxial, non-isochoric hardening behavior respective to the experimental tensile, compression and shear data.

For PP the effective stress notion was employed in conjunction with a damage parameter assessed on the relation with the true stress values. Good results were obtained for the damage behavior at different stress states in the miniflat and notched tensile tests. For PC another approach was presented using the yield point after Considère to reflect the plastic strain as realistic as possible. The experimental, local deformation behavior could be matched in the simulations by using the true stress values as input. To predict the load drop in the various tensile tests a non-linear, stress triaxiality dependent damage evolution law by employing the GISSMO model is suggested. However, it is particularly difficult to predict the load drop on the specimen level. For the simulation of a component the calibrated model is suitable to describe the global force-displacement response.

The failure locus could be determined in a straightforward manner via a combined experimental-numerical approach by using an average triaxiality factor. An exemplary quadratic failure curve was fitted for a strain rate of 10 s⁻¹. Element size regulation and strain rate dependency of the failure strains were not considered in this work.

The calibrated models represent the experimental material behavior to a high degree. Benchmark tests of components for validation are planned for future studies. Non-linear damage evolution and strain rate dependent failure of thermoplastic polymers are as well of interest for further investigations. However, there are still simplifications of the real behavior to the present models:

1. Until yield point the model is linear elastic (viscoelastic behaviour of polymers).
2. Rate effects in compression and shear are assumed to be equal to the strain rate dependency of the tensile data.
3. Temperature dependency is not taken into account (adiabatic heating under impact loading of PC).
4. Anisotropic effects due to the morphological structure are neglected.
5. Biaxial tensile test data could improve the results accounting for stress induced crazing.
6. More stress states need to be covered to validate the quadratic failure curve (or to find another fit function).

Keeping these simplifications in mind accurate results can be obtained by the presented model calibration methodology.

7 Literature

[1] Lin, S.; Xia, Y., and Lin, C.-H.: "Stress state dependent failure loci of a talc-filled polypropylene material under static loading and dynamic loading ", ICF13, 2013

[2] Lobo, H.; Croop, B., and Roy, D.: "Applying Digital Image Correlation Methods to SAMP-1 Characterization", 9th European LS-DYNA Conference, Manchester, 2013

[3] Nutine, M.; Vitali, M.: " Characterization of Polyolefins for Design Under Impact: from True Stress/Local Strain Measurements to the FE Simulation with LS-Dyna Mat. SAMP-1", 7. LS-DYNA Anwenderforum, Bamberg, 2008

[4] Daiyan, H. et al.: "Numerical simulation of low-velocity impact loading of polymeric materials ", 7th European LS-DYNA Conference, Salzburg, 2009

[5] Bao, Y. and Wierzbicki, T.: "On fracture locus in the equivalent strain and stress triaxiality space", International Journal of Mechanical Sciences 46.1, 2004, pp. 81-98

[6] Effelsberg, J. et al.: "On parameter identification for the GISSMO damage model", 12th International LS-DYNA Users Conference, Dearborn, 2012

[7] Takekoshi, K. and Niwa, K.: "A Study on Preparation of Failure Parameters for Ductile Polymers", 13th International LS-DYNA Users Conference, Detroit, 2014

[8] Jerabek, M.; Major, Z., and Lang, R.: "Advanced Characterization of the Tensile and Compressive Behavior of PP and PP Composites ", Dissertation at the University of Leoben, Austria, 2009

[9] G'sell, C. and Jonas, J. J.: "Determination of the plastic behaviour of solid polymers at constant true strain rate", Journal of Materials Science 14.3, 1979, pp. 583–591

[10] Reiter, M. and Major, Z.: "Determination of Tensile Properties of Polymers at High Strain Rates", EPJ Web of Conferences 6, 2010, p. 39008

[11] Jerabek, M. et al.: "Multiaxial yield behaviour of polypropylene", EPJ Web of Conferences 6, 2010, p. 03005

[12] Considère, A.: "L'emploi du fer et de l'acier, dans les constructions", Annales des Ponts et Chaussées 9.2, 1985, pp. 574–775

[13] Quinson, R. R.; Perez, J.; Rink, M. et al.: "Yield criteria for amorphous glassy polymers", Journal of Materials Science 32.5, 1997, pp. 1371–1379

[14] Merklein, M. and Biasutti, M.: "Forward and reverse simple shear test experiments for material modeling in forming simulations", Steel Research International, Special Edition ICTP, 2001, pp. 702–707

[15] Kolling, S. et al.: "SAMP-1: A Semi-Analytical Model for the Simulation of Polymers", 4. LS-DYNA Anwenderforum, Bamberg, 2005

[16] Sarva, S. and Boyce, M.: "Mechanics of polycarbonate during high-rate tension", Journal of Mechanics of Materials and Structures, 2007, pp. 1853–1880

[17] Takekoshi, K. and Niwa, K.: "Validation and material modeling of polymers by employing MAT_SAMP-1", 12th International LS-DYNA Users Conference, Detroit, 2012

[18] Lemaitre, J.: "A continuous damage mechanics model for ductile fracture", Journal of Engineering Materials and Technology 107.1, 1985, pp. 83–89

[19] Hayashi, S.: "Prediction of failure behaviors in polymers under multiaxial stress state", 12th International LS-DYNA Users Conference, Detroit, 2012